THE JOURNAL OF BIOLOGICAL CHEMISTRY VOL. 285, NO. 14, pp. 10690–10702, April 2, 2010

Translational Regulation of Gene Expression by an Anaerobically Induced Small Non-coding RNA in *Escherichia coli*[*] [S]

Received for publication, November 27, 2009, and in revised form, January 12, 2010 Published, JBC Papers in Press, January 14, 2010, DOI 10.1074/jbc.M109.089755

Anders Boysen, Jakob Møller-Jensen, Birgitte Kallipolitis, Poul Valentin-Hansen[1], and Martin Overgaard

From the Department of Biochemistry and Molecular Biology, University of Southern Denmark, 5230 Odense M, Denmark

Small non-coding RNAs (sRNA) have emerged as important elements of gene regulatory circuits. In enterobacteria such as *Escherichia coli* and *Salmonella* many of these sRNAs interact with the Hfq protein, an RNA chaperone similar to mammalian Sm-like proteins and act in the post-transcriptional regulation of many genes. A number of these highly conserved ribo-regulators are stringently regulated at the level of transcription and are part of major regulons that deal with the immediate response to various stress conditions, indicating that every major transcription factor may control the expression of at least one sRNA regulator. Here, we extend this view by the identification and characterization of a highly conserved, anaerobically induced small sRNA in *E. coli*, whose expression is strictly dependent on the anaerobic transcriptional fumarate and nitrate reductase regulator (FNR). The sRNA, named FnrS, possesses signatures of base-pairing RNAs, and we show by employing global proteomic and transcriptomic profiling that the expression of multiple genes is negatively regulated by the sRNA. Intriguingly, many of these genes encode enzymes with "aerobic" functions or enzymes linked to oxidative stress. Furthermore, in previous work most of the potential target genes have been shown to be repressed by FNR through an undetermined mechanism. Collectively, our results provide insight into the mechanism by which FNR negatively regulates genes such as *sodA*, *sodB*, *cydDC*, and *metE*, thereby demonstrating that adaptation to anaerobic growth involves the action of a small regulatory RNA.

In recent years non-coding RNAs have emerged as important components of regulatory circuits both in bacteria and eukaryotes (1–3). In enteric bacteria such as *Escherichia coli* and *Salmonella* more than a hundred different sRNAs[2] have been identified, and a major class consists of trans-encoded gene regulatory RNAs that act by an antisense mechanism to activate or, more frequently, to repress translation of target mRNAs. Many of these sRNAs are conserved in related species, are made in response to changes in environmental conditions, and are required for adaptation to stress or specific growth conditions. Several common features have been uncovered. First, the sRNA genes are generally highly regulated at the transcriptional level and are frequently expressed as components of global regulatory systems. Well studied regulatory cases include OxyR regulation of OxyS RNA (oxidative stress) (4), Fur regulation of RyhB RNA (iron limitation) (5), cAMP-CRP regulation of CyaR and Spot 42 RNA (glucose limitation) (6–9), OmpR regulation of MicF, OmrA, and OmrB RNAs (osmotic shock) (10, 11), σ^E-mediated transcription of MicA and RybB RNAs (envelope stress) (2, 12), PhoPQ regulation of MgrR (Mg^{2+}/Ca^{2+} transport and virulence) (13), and LuxO control of Qrr1–4 (quorum sensing in *Vibrio*) (14). Furthermore, small RNA expression may be under control of a dedicated transcription factor, as exemplified by SgrR/SgrS RNA (glucose-phosphate stress) (15). Second, pairing typically occurs at or near the ribosome binding site of the target mRNA, leading to translational inhibition and concomitant rapid coupled degradation of sRNA-mRNA duplexes in a degradosome-dependent manner (16, 17). Such features provide rapid ON/OFF regulatory mechanisms and, hence, are ideally suited as reversible switches responding to stress signals. Moreover, the sRNAs often regulate multiple targets via limited complementarity, and frequently a highly conserved exposed portion of the regulatory RNA is used for pairing. Finally, all the trans-acting base-pairing RNAs characterized thus far in *E. coli* and *Salmonella* associate with and require the RNA chaperone Hfq, the bacterial equivalent of eukaryotic Sm-like proteins (18). *In vivo*, the protein stabilizes most of the base-pairing RNAs. Moreover, Hfq facilitates the base-pairing between sRNAs and their target mRNAs and strongly enhances the on-rate of duplex formation *in vitro* (7, 16, 19–22). Because Hfq possesses distinct binding surfaces for U-rich and AG-rich tracks of RNA, it seems likely that the protein serves as a docking platform to bring RNA partners in close proximity, thereby increasing the likelihood of annealing (22–25).

So far, no anaerobically induced small RNA has been identified or predicted in *E. coli*. At the level of transcription, the

* This work was supported by the Danish National Research Foundation (Grundforskningsfonden), The Lundbeck Foundation, and the Danish Natural Science Research Council.

[S] The on-line version of this article (available at http://www.jbc.org) contains supplemental Tables S1–S4 and Fig. 1.

[1] To whom correspondence should be addressed: Campusvej 55, DK-5230 Odense M, Denmark. Tel.: 45-6550-2375; Fax: 45-6550-2467; E-mail: valentin@bmb.sdu.dk.

[2] The abbreviations used are: sRNA, small regulatory RNA; ArcA, regulator of aerobic respiratory control; CAP, the catabolite gene activator protein; FNR, regulator of fumerate and nitrate reduction; Fur, ferric uptake regulator; TIR, translational initiation region; IGR, intergenic regions; SOD, superoxide dismutase; GFP, green fluorescent protein; fw, forward; rv, reverse; DTT, dithiothreitol; Bis-Tris, 2-[bis(2-hydroxyethyl)amino]-2-(hydroxymethyl)propane-1,3-diol; CHAPS, 3-[(3-cholamidopropyl)dimethylammonio]-1-propanesulfonic acid; MALDI-TOF/TOF, matrix-assisted laser desorption ionization time-of-flight.

adaptive response to anoxia or to O_2-limited environments is coordinated by two global regulators, the FNR protein and the Arc two-component system, comprising the ArcB sensor kinase and the ArcA response regulator (26). The two systems are intimately linked through the genes controlled by both regulators and the FNR-mediated activation of *arcA* expression (27). Both systems become activated in response to anaerobiosis, but whereas FNR is a direct O_2 sensor via an oxygen sensitive $[4Fe\text{-}4S]^{2+}$ cluster, ArcB senses O_2 availability indirectly by monitoring the redox state of the quinone pool (28–30). Furthermore, the regulatory outcome is essentially reciprocal in that FNR usually activates transcription, whereas ArcA generally acts as a negative regulator. FNR is a structural and functional homolog of CAP (the catabolite gene activator protein, also known as CRP), and their DNA binding sites are sufficiently similar to envisage joint occupation (26, 31). Regulatory studies along with genome-wide expression approaches have shown that FNR, directly or indirectly, controls the expression of numerous gene products in *E. coli* (>200) (32–35). A major consequence of the FNR-mediated regulation of gene expression upon switching to anaerobic growth conditions is a reprogramming of energy metabolism to utilize alternative mechanisms of energy conservation in the absence of O_2 as the terminal electron acceptor. Furthermore, FNR represses the expression of genes that are needed for aerobic metabolism (26).

In this work we report on the identification and characterization of a highly conserved, anaerobically induced sRNA in *E. coli*, whose expression is strictly dependent on FNR. In keeping with the naming of the OxyR- and SgrR-regulated small regulatory RNAs (*i.e.* OxyS and SgrS), it was designated FnrS (FnR-regulated sRNA). This novel sRNA possessed hallmarks of base-pairing RNAs, and genome-wide expression approaches identified multiple candidate target RNAs. We validated a number of these candidates by various experimental approaches, including Northern blot analysis and specialized reporter plasmids for studying post-transcriptional control of gene expression, and compared our data with previous studies of FNR-mediated control of gene expression. Specifically, a number of unexplained regulatory observations around FNR-mediated repression of gene expression can now be understood in light of our studies of the FNR-dependent sRNA.

EXPERIMENTAL PROCEDURES

Media, Antibiotics, Strains, and Plasmid—Luria-Bertani (LB), 2× yeast extract/Tryptone medium (36), and minimal medium (37) supplemented with either 0.2% glucose or 0.2% glycerol were prepared as described. When required, the media were supplemented with 30 or 100 μg/ml ampicillin, 40 μg/ml chloramphenicol, and 40 μg/ml kanamycin. Protein expression was induced from the $P_{A1/O4/O3}$ promoter by 1 mM isopropyl-β-D-thiogalactopyranoside (IPTG). All strains used were derivatives of *E. coli* K-12. Strains and plasmids are listed in supplemental Table S1, and primers are in supplemental Table S2.

Construction of Strains—The *fnrS* knock-out strain was made by replacing the *fnrS* gene with a chloramphenicol resistance cassette as described by Datsenko and Wanner (38). Briefly, a PCR amplification product generated using pKD3 as template and the primers Δ-*fnrS*-fw and Δ-*fnrS*-rv was electroporated into SØ928. Electroporants were selected and isolated. The SØ928 Δ*fnr*::*kan* strain as well as the SØ928 Δ*arcA*::*kan* strain was constructed by P1 phage transduction. Markerless (chloramphenicol- or kanamycin-sensitive) SØ928 Δ*fnrS*, SØ928 Δ*arcA*, and SØ928 Δ*fnr* strains were made by flipping out the integrated antibiotic resistance cassette using pCP20 (38). All constructs were verified by PCR analysis. The primers fnrS −139 and fnrS +118, FNR −191 (forward) fw and FNR +921 (reverse) rv, and arcA fw and arcA rv were used to verify Δ*fnrS*, Δ*fnr*, and Δ*arcA*, respectively.

Plasmids—Plasmid pAB1000 was derived from pNDM220 (39) by digesting a PCR product with AatII and BamHI and subsequent ligation into the same sites of pNDM220. The PCR product was generated by using the primers AatII PA1O4 fnrS and BamHI 3′ fnrS on SØ928 chromosomal DNA. Plasmid pAB1001 was derived from pMG25 by partial digestion of a PCR product with EcoRI and BamHI and subsequent ligation into the same sites of pMG25. The PCR product ligated into pMG25 was generated in two steps. In the first step the PCR fragments A and B were generated by using chromosomal SØ928 DNA as the template. The primers pMG25_fnr1 and Fnr D154A rv were used to introduce an EcoRI site and the D154A point mutation in the PCR fragment in the extreme 3′ end. The PCR product, which contained the D154A point mutation in the extreme 5′ end and a His_6 in the 3′ end as well as a BamHI site was made by using the primers Fnr D154A fw and pMG25_fnr2-His6. In the second step the two PCR fragments containing overlapping sequences in the 3′ and 5′ ends, respectively, were used as the template, and the primers pMG25_fnr1 and Fnr D154A fw were used to synthesize the final PCR product. All plasmid modifications were verified by DNA sequencing. To study the FnrS-mediated translational control on a number of mRNA targets, we have used the green fluorescent protein (GFP)-based reporter system developed by Urban and Vogel (40). Briefly described, the full-length 5′-untranslated region and 30 bp of the N-terminal coding region of *metE*, *sodA*, *sodB*, and *yobA* was amplified by PCR and subsequently fused translationally to the 5′ terminus of GFP in the pXG-10 vector. This in turn generated the plasmids pAB1002 (*metE′*::*gfp*), pMO99 (*sodA′*::*gfp*), pMO101 (*sodB′*::*gfp*), and pAB1005 (*yobA′*::*gfp*). The relevant primer pairs are listed in supplemental Table S2. All constructs were verified by DNA sequencing using the primers pZE-CAT and pJVO-155 to amplify the region of interest.

Protein Expression and Purification—The *E. coli* Hfq protein was expressed and purified as described (7). Strain AB102 was used to overexpress FNR D154A-His_6. Briefly, strain AB102 was grown at 37 °C in 500 ml of LB with appropriate antibiotics until an A_{450} of 0.5. Expression of the His-tagged protein was induced by the addition of 1 mM IPTG for 4 h. Cells were harvested, resuspended in 15 ml of lysis buffer (50 mM sodium phosphate, pH 7.0, 300 mM NaCl) supplemented with Complete protease inhibitor mixture (Roche Applied Science), and lysed three times in a French press at 10.000 p.s.i. Lysate was cleared by centrifugation at 20,000 rpm for 45 min at 4 °C. The cleared supernatant was loaded onto a TALON His-tag Affinity

Resin (Clontech) column, and the protein was purified under native conditions as recommend by manufacturer. The eluate was dialyzed against phosphate-buffered saline buffer containing 10% glycerol and subsequently stored at −80 °C.

Transcriptome Analysis—Global gene expression analysis was carried out using *E. coli* glass-slide microarrays (*E. coli* K-12 V2 OciChip, Ocimum Biosolutions) as previously described (20). In brief, strains SØ928/pNDM220 (control) and SØ928/pAB1000 carrying an ectopic copy of the sRNA gene under the control of the inducible $P_{A1/O4}$ promoter were grown in LB medium to early exponential phase and induced with 1 mM IPTG for 10 min. In a parallel experiment wild-type and SØ928 Δ*fnrS* were grown aerobically to early exponential phase after which the growth condition was changed to anoxic for 30 min by incubation in an air tight tube without agitation or air. Total RNA from the four strains was extracted, and Cy3- and Cy5-labeled cDNA probes were synthesized. Probe synthesis and hybridization was carried out as described (20). Each experimental condition was performed as three independent biological replicates, and each replicate included a dye swap replication. Background-subtracted fluorescence intensity data were subjected to further analysis using the TM4 microarray software suite (41). In short, the data sets were subjected to Lowess print-tip normalization and further intensity-filtered. Only genes passing a One Class *t* test (p value <0.05) were considered in the initial analysis. Genes whose expression were negatively regulated by FnrS were selected by the criterion that they exhibited a decreased expression ratio upon FnrS overproduction and an increased expression ratio in an *fnrS* deletion strain during anaerobic growth conditions. Vice versa, genes whose expression were positively regulated by FnrS were selected by the criterion that they exhibited an increased expression ratio upon FnrS overproduction and a decreased expression ratio in an *fnrS* deletion strain during anaerobic growth conditions.

Northern Blot Analysis—Total RNA extraction and Northern blot analyses were done as described (42). FnrS and the target mRNAs *sodA* and *sodB* as well as *metE′*::*gfp*, *sodA′*::*gfp*, *sodB′*::*gfp*, and *yobA′*::*gfp* constructs were detected using γ-^{32}P end-labeled DNA oligos (supplemental Table S2).

Half-life Determination of FnrS—Cells were grown aerobically to an A_{450} of 0.4, and then growth was continued under anaerobic conditions for 20 min to induce expression of FnrS. At this point the culture was poured into 15-ml tubes containing 300 μg/μl rifampicin (final concentration). To maintain anaerobic growth conditions, the tubes were filled to the very top and sealed with butyl rubber plugs. At the indicated times, each sample was chilled in liquid nitrogen and collected by centrifugation at 0 °C. The expression level of FnrS was monitored upon a shift from anaerobic to aerobic conditions. In brief, wild-type cells were grown anaerobically for 120 min after which the culture was vigorously aerated. Samples were collected and treated as described above. To determine the half-life of FnrS induced under aerobic conditions, strain SØ928 Δ*fnrS*/pNDM220-fnrS was grown under aerobic conditions to mid-exponential phase (A_{450} = 0.4) after which IPTG (1 mM final concentration) was added to the culture. After 20 min of induction, synthesis from the $P_{A1/O4/O3}$ promoter was terminated by harvesting and resuspending the cells in an equal volume of prewarmed medium supplemented with 0.2% glucose to wash out the inducer. At the indicated times each sample was chilled in liquid nitrogen and collected by centrifugation at 0 °C. In all three experiments the extracted RNA was analyzed by Northern blotting as described. The intensities were normalized and plotted, and the RNA half-life was subsequently calculated using the slope from each plot.

Primer Extension Analysis—Primer extension analysis was carried out according to Franch *et al.* (43). To map the *fnrS* transcription start site, primer *fnrS* RT-primer #1 was used for the reverse transcription reaction (supplemental Table S2). The sequence ladder was synthesized using a PCR template generated by using primers *fnrS* −139, *fnrS* +118, and SØ928 chromosomal DNA as template. Primers cydD-pxt+32-r and cydD pxt+70-r were used to map and analyze the expression of the *cydDC* 5′ end, whereas cydD-pxt-169-f was used as forward primer for the synthesis of the sequence ladder.

Electrophoretic Mobility Shift Assays—All binding assays was carried out in a 10- or 20-μl standard reaction in 1× binding buffer and incubated for 20 min at 37 °C before the addition of 5 μl of loading buffer (5% glycerol, 0.1% xylene cyanol). The samples were subsequently subjected to native PAGE on 5% polyacrylamide gels at 4 °C in 0.5× TBE (0.05 M Tris-HCl, pH 8.4, 0.045 M boric acid 0.005 M EDTA). Gels were subjected to phosphorimaging or direct fluorescent scanning on a Typhoon Trio scanner (GE Healthcare). Binding of Hfq protein to FnrS RNA was carried out in 1× Hfq binding buffer (20 mM HEPES, pH 8, 100 mM KCl, 1 mM $MgCl_2$, 1 mM DTT) using 4 nM of ^{32}P 5′ end-labeled FnrS and increasing amounts of Hfq in the presence of a 500-fold molar excess of *E. coli* tRNA (Roche Applied Science) in a 10-μl total volume. To analyze the interaction of FNR D154A-His_6 to P_{fnrS}, a Cy5 end-labeled PCR product covering 147 bp upstream and 47 bp downstream of the transcription start site of *fnrS* was generated using the primers *fnrS* −147 fw and *fnrS* +47 rv. Relevant amounts of purified FNR D154A-His_6 were incubated with a total of 2 nM P_{fnrS} DNA probe in 1× FNR binding buffer (20 mM Tris-HCl, pH 7.5, 100 mM KCl, 2 mM $MgCl_2$, 1 mM DTT, 50 μg/μl bovine serum albumin) under standard binding conditions (20 μl volume) supplemented with 0.1 mg/ml sonicated salmon sperm DNA. A PCR product (primers *narK* −150 fw and *narK* +63) covering 150 bp upstream and 63 bp downstream of the transcription start site of *narK* was used as a positive binding control (44). The *E. coli relBE* promoter-operator fragment $relO_{166}$ was used as a control for specificity (45). Hfq-sRNA-mRNA interactions were carried out in 1× Hfq binding buffer (20 mM HEPES, pH 8, 100 mM KCl, 1 mM $MgCl_2$, 1 mM DTT) using 2 nM ^{32}P 5′ end-labeled FnrS, 2 μM tRNA either in the presence or absence of 0.33 μM Hfq (hexamer concentration) and relevant amounts of either *sodA* or *sodB* in a total volume of 10 μl.

In Vitro Synthesis and Labeling of RNA—The *sodA* and *sodB* RNA probes and FnrS were prepared by *in vitro* transcription (MegaScript, Ambion) with 1 μg of PCR template as the input DNA. The FnrS, *sodA*, and *sodB* PCR products were obtained by using SØ928 chromosomal DNA as the template and the primer sets *fnrS* T7 fw and *fnrS* T7 rv, *sodA* T7 fw and *sodA* T7 rv, and *sodB* T7 fw and *sodB* T7 rv, respectively. Each *in vitro* transcript was DNase I-treated before PAGE separation on a 6%

8 M urea denaturing gel. The RNAs were extracted from the gel and quantified on a NanoDrop 1000 (Thermo Scientific). If required, the transcripts were radiolabeled at the 5′ end with [γ-^{32}P]ATP using the KinaseMax kit (Ambion).

One-dimensional SDS-PAGE and Western Blot—Culture samples were grown under either aerobic or anaerobic conditions for six generations to A_{450} = 0.4 if not stated otherwise. The cell pellet was resuspended in 1× SDS loading buffer (60 mM Tris-HCl, pH 6.8, 2% SDS, 10% glycerol, 0.005% bromphenol blue, 5 mM EDTA, 0.1 M DTT) to a final concentration of 3×10^6 cells/μl. Whole-cell protein fractions were boiled for 5 min and separated on a 12% Tris-glycine SDS-polyacrylamide gel. Proteins were visualized by silver staining as described by the Vorum silver-staining protocol modified for mass spectrometry as described in Mortz *et al.* (46). For detection of GroEL and GFP fusion constructs, total protein from 1.5×10^7 cells was loaded onto 4–12% Invitrogen NuPage novex Bis-Tris mini gels. The gels were blotted for 60 min at 0.8 mA/cm^2 in a Hoefer SemiPhor blotter tank (Amersham Biosciences) onto a polyvinylidene difluoride membrane (Millipore) in transfer buffer (48 mM Tris, pH 9, 20% methanol, 39 mM glycine, 0.0375% SDS). The protein membranes were handled using a SNAP inner diameter protein detection system (Millipore) as recommended by the manufacturer. The α-GFP (Roche Applied Science) and α-GroEL (Sigma) monoclonal antibodies were diluted either 1:100,000 or 1:20,000, respectively. Mouse and rabbit horseradish peroxidase-conjugated secondary antibody was diluted 1:2000 (DakoCytomation). Blots were developed using Western lightning reagent (PerkinElmer Life Sciences). The signal was detected and quantified using the Quantity One software associated with the ChemiDoc XRS station (Bio-Rad).

[^{35}S]Methionine Pulse Labeling and Two-dimensional Gel Electrophoresis—Strains SØ928ΔfnrS/pNDM220 and SØ928Δ*fnrS*/pNDM220-fnrS were grown in minimal medium supplemented with 0.2% glucose. Exponentially growing cultures (A_{450} = 0.3) were induced with 0.5 mM IPTG for 30 min before [^{35}S]methionine pulse-labeling. Samples (2 ml) were labeled with 20 μCi of carrier-free [^{35}S]methionine and incubated at 37 °C for 2 min followed by a chase with unlabeled methionine (0.2 mg/ml) for 1 min. The chase was terminated by the addition of 5 μl of chloramphenicol (50 mg/ml) to stop protein synthesis. Cells were collected by centrifugation at 0 °C and lysed by sonication in sonication buffer (50 mM Tris-HCl, pH 8.8, 50 mM KCl, 5 mM β-mercaptoethanol) supplemented by Complete protease inhibitor mixture (Roche Applied Science). The proteins were precipitated by ethanol/acetone precipitation and resuspended in IPG buffer (7 M urea, 2 M thiourea, 2% CHAPS, 0.4% DTT, 0.5% Pharmalyte 3-10, 0.5% IPG 6–11 buffer). Two-dimensional gel electrophoresis was carried out according to Rogowska-Wrzesinska *et al.* (47). Protein samples containing equal amounts of total [^{35}S]methionine radioactivity (5×10^6 cps) were loaded onto first-dimension gel strips for in-gel rehydration (18-cm Immobiline Drystrip, pH 4–7, GE Healthcare) and subjected to isoelectric focusing. Second-dimension gel electrophoresis was performed using a Protean II XL system (Bio-Rad) and laboratory-made 12.5% (w/v) acrylamide gels (acrylamide: N:Nk-ethylene-bisacrylamide ratio 200:1). Gels were finally dried and subjected to phosphorimaging.

Mass Spectrometry—Protein spots of interest were excised from one- and two-dimensional gels and placed in MilliQ water. The proteins were in gel-digested as described by Prokhorova *et al.* (48). Peptide mass fingerprints and MALDI-TOF/TOF spectra were obtained on an UltraFlex MALDI-TOF/TOF instrument (Bruker Daltonics). All peptide mass fingerprints were two-point internally calibrated using known masses of tryptic peptides and annotated by the Bruker Daltonics flexAnalysis software Version 2.2. The data were searched against the NCBInr data base in the entries for eubacteria using an in-house MASCOT server (Matrix Science). Peptide tolerance was set to 120 ppm for peptide mass fingerprints and 0.9 Da for MALDI-TOF/TOF spectra. Cysteine carbamidomyalation was set as a fixed modification. Methionine oxidation was set as a variable modification. One missing cleavage was allowed per peptide. For positive protein identification the score of the result of ($\times 10 \log p$) had to be over the significance threshold level (p, 0.05). However, if the score was below the significance threshold, a number of criteria were used, *i.e.* (i) identification of the organism of interest, (ii) theoretical size of the data base hit *versus* the observed size in the one-dimension gel, and (iii) manual analysis of the quality of the TOF/TOF spectrum.

RESULTS

Identification of FnrS RNA and Characterization of Its Expression Pattern—As a starting point for detecting putative FNR-controlled sRNAs in *E. coli*, we considered a number of common properties of previously identified sRNAs. First, the non-coding RNA transcripts range in average from 50 to 250 nucleotides in length, and the sRNA-encoding genes are located primarily in intergenic regions (IGR). Second, they are generally produced as single transcripts, and transcription normally terminates with a Rho-independent terminator consisting of a base-paired hairpin followed by a string of U residues. We, therefore, carried out searches for sequences in IGRs of the *E. coli* genome that contain a near consensus DNA binding site for FNR followed by a potential termination signal and that are separated by 100–350 bp. Specifically, a simple pattern search at the Colibri Web Server for sequences possessing the underlined part of the FNR consensus binding motif, 5′-TTGATN$_4$ATCTT-3′ and ending with a string of seven T residues resulted in a single candidate sRNA gene localized in the *ydaN-dbpA* IGR (Fig. 1*A*). Intriguingly, on the basis of high conservation, an sRNA candidate has been predicted to be encoded in this IGR (designated RydA), but no expression was detected by gene array or Northern blot analysis (49). Furthermore, the promoter region of the candidate gene has been identified as a strong target for FNR in a study that investigated the binding of this global regulatory protein for anaerobic metabolism across the entire *E. coli* chromosome (50). In addition, an Hfq-bound sRNA species in the same IGR was identified recently in a deep sequencing study of Hfq-bound RNAs in *Salmonella* (gene STnc580) (51).

To verify that *fnrS* transcription is indeed controlled by FNR, we analyzed by Northern blot the expression profile of this

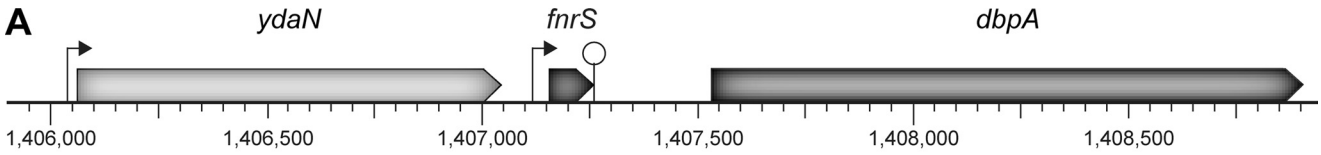

B

```
                    FNR site                                  -10      5´→ fnrS
ECO  AAAAACGCCGCAAAGTTTGAGCGAAGTCAATAAACTCTCTACCCATT-CAGGGCAATATCTCTCTTGCAGGTGAAT
KPN  GAAAACCCGGCAATGTTTGAGCGAAATCAATAAACCATCTACCCATT-CAGGGCAATATCTCTCTCGCAGGTGAAT
STY  AAAAACGCCGAGAAATTTGAGCGAAGTCAATAAACCATCTACCTATT-CGGGGCAATATCTCTCTCGCAGGTGAAT
CRO  AAAAAGGGCTTTTAAATTGAGCGAAGTCAATAAACGTCACGCCTGTT-CGCGGCAATATCACTCTCGCAGGTGAAT
SGL  CTTTTTGGCTCCAAAATTGAGCAATATCAATAATA-GTGATCGCAATATGAGGCATGATCACTTCCGCAGGTGAAT
YPE  ATTAGTCACCGAAAAATTGAGCCACATCAAGACTTTGTTGTGGTGGC-TCAGGCATGATTA-TTTTGCAGGTGAAT
Edw  AAAAGCGCGGAGGAAATTGAGCGATATCAAACTTCACTCGAAGTAGG-TAGGGCAAACTTCATTTCGCAGGTGAAT
SMA  GAAAACCCGGTTAACATTGAGCAAAATCAACATTTAGCCGGGGGAAA-TGGGGCATGATCTCTCTCGCAGGTGAAT
DDA  AAAACCATTGTTAATATTGAGCAATATCAACATTTCCGAGACATGCT-TGCGGCACTATCCCTCCCGCAGGTGAAT
ESA  AAAAATCCTCACGACTTTGAGCGATATCAAGAAATGGTACGTCGTTT-CACGGCATCATTCTTGTCGCAGGTGAAT
CTU  AAAAAACCTCACGAGTTTGAGCGACATCAAGAAATGGTACGCCGTTT-CACGGCATCATTCCTGTCGCAGGTGAAT
PMI  AATTCTCTAACTCTGTTTGAGATATATCAATTTTTTAAATGCCAACA-TCTGGCATTATAACTCTCGCAGGTGAAT
PHO  AAAACTAGTTTCTAATTTGAGATATATCAATGTTCATCAAGAATACT-TCAGGCATTATGACTCCCGCAGGTGAAA
PST  GTTAACCCACCCTTGTTTGAGATAAATCAATAAAAGGTACGTTGATT-TGGGGCACTATTAATTCCGCAGGTGAAT
                *****  *  ****                ****   *   *   *********
```

FIGURE 1. **Schematic organization of the *fnrS* chromosomal region and conservation of the promoter region.** *A*, genetic organization of the *E. coli* region encoding *fnrS* is shown. *Arrows* indicate the direction of transcription, and stem-loop structures of the predicted ρ-independent terminator are indicated by a *lollipop*. The *fnrS* gene is highly conserved in a wide range of enterobacteria. *B*, alignment of the *fnrS* promoter region of *E. coli* K-12 (*ECO*), *Klebsiella pneumoniae* (*KPN*), *Salmonella typhimurium* (*STY*), *Citrobacter rodentium* (*CRO*), *Sodalis glossinidius* (*SGL*), *Yersinia pestis* (*YPE*), *Edwardsiella* (*EDW*), *Serratia marcescens* (*SMA*), *Dickeya dadantii* (*DDA*), *Enterobacter sakazakii* (*ESA*), *Cronobacter turicensis* (*CTU*), *Proteus mirabilis* (*PMI*), *Photorhabdus asymbiotica* (*PHO*), and *Providencia stuartii* (*PST*) by the ClustalW program. The −10 promoter element and the FNR DNA binding site are *highlighted* in *gray*. The transcription start site of the *E. coli fnrS* gene is indicated by an *arrow*.

sRNA in cells cultured under aerobic or anaerobic growth conditions ($+O_2$ or $-O_2$) and under anaerobic growth conditions in the presence or absence of FNR. The results presented in Fig. 2*A* show that expression of FnrS occurs in wild-type cells only under anaerobic growth conditions. Within 20 min after a sudden shift to anaerobic growth (time 0) the cellular level of the sRNA increased >100-fold. Furthermore, the anaerobic transcription of *fnrS* was abolished in a Δ*fnr* strain, thus demonstrating that the global regulatory protein FNR induces FnrS transcription in response to anoxic growth conditions. Because ArcA operators are poorly defined and because of potential overlap between FNR and CAP DNA binding sites, we also examined anaerobically induced FNR production in *arcA* and *crp* deletion strains. As shown in Fig. 2*A*, *lower panels*, *fnrS* transcription is switched on in a manner quite similar to that seen for the wild type, but initially the induction is somewhat delayed by each mutation. In this regard we note that the two mutant strains grew slower than the parental strain, indicating that it takes more time for the ArcA- and CAP-deficient cells to deplete the medium for oxygen after a sudden shift to anaerobic growth. Therefore, the reduction in initial transcription might be attributed to the growth rate rather than to a direct effect of ArcA/CAP.

We confirmed by electrophoretic mobility shift assays that FNR associates with the near FNR consensus binding motif of *fnrS* (data not shown), and primer extension analyses of FnrS RNA showed that the 5′ end most likely corresponds to bp 1.407.153 of the *E. coli* chromosome (Fig. 2*B*). Thus, the FNR binding site is located at a proper distance for activation (*i.e.* −42.5), and a potential σ^{70} Pribnow box (CAATAT) for this initiation point was detected as well (Fig. 1*B*). Furthermore, these sequence elements are conserved in putative *fnrS* gene of other enterobacterial species (Fig. 1*B*). Assuming that *fnrS* transcription terminates at the terminal uridine of the predicted Rho-independent terminator (corresponding to position 1.407.274 of the *E. coli* chromosome), the length of FnrS is 122 nucleotides, which is in perfect agreement with the ~120-nucleotide RNA detected in Northern blot analysis. The FnrS secondary structure, as predicted by the folding program Mfold, is shown in Fig. 2*C*.

Role of Hfq and Turnover of FnrS—The Hfq protein has been found to be necessary for the action of many trans-encoded sRNAs and, as mentioned, was reported to interact with *Salmonella* FnrS in immunoprecipitation experiments (51). To confirm these data, we examined the ability of the RNA chaperone to associate with the sRNA using gel-shift assays. The results presented in Fig. 3*A* show that hexameric Hfq binds fairly well to FnrS (apparent $K_D \sim 0.03$ μM). Accordingly, the sRNA bears a typical recognition site for Hfq around position 60, consisting of a single-stranded U-rich track flanked by a hairpin (Fig. 2*C*).

Given that Hfq is important for the stability of many of the small regulatory RNAs, we next determined the half-life of FnrS in the presence or absence of Hfq. To this end anaerobically grown cells were treated with the transcription inhibitor rifampicin, and aliquots of cells were taken for Northern blot analysis at different intervals after the addition of the drug (Fig. 3*B*). In the wild-type strain, FnrS was very stable (half-life ~ 100 min), whereas the stability of the small RNA was dramatically decreased (~15-fold) in a mutant strain background deleted for *hfq* (Fig. 3*B*). This is consistent with what has been reported for other RNAs (*e.g.* Spot 42, RyhB, and MicM) (7, 17, 20) and indicates that Hfq also associates with FnrS *in vivo*, thereby

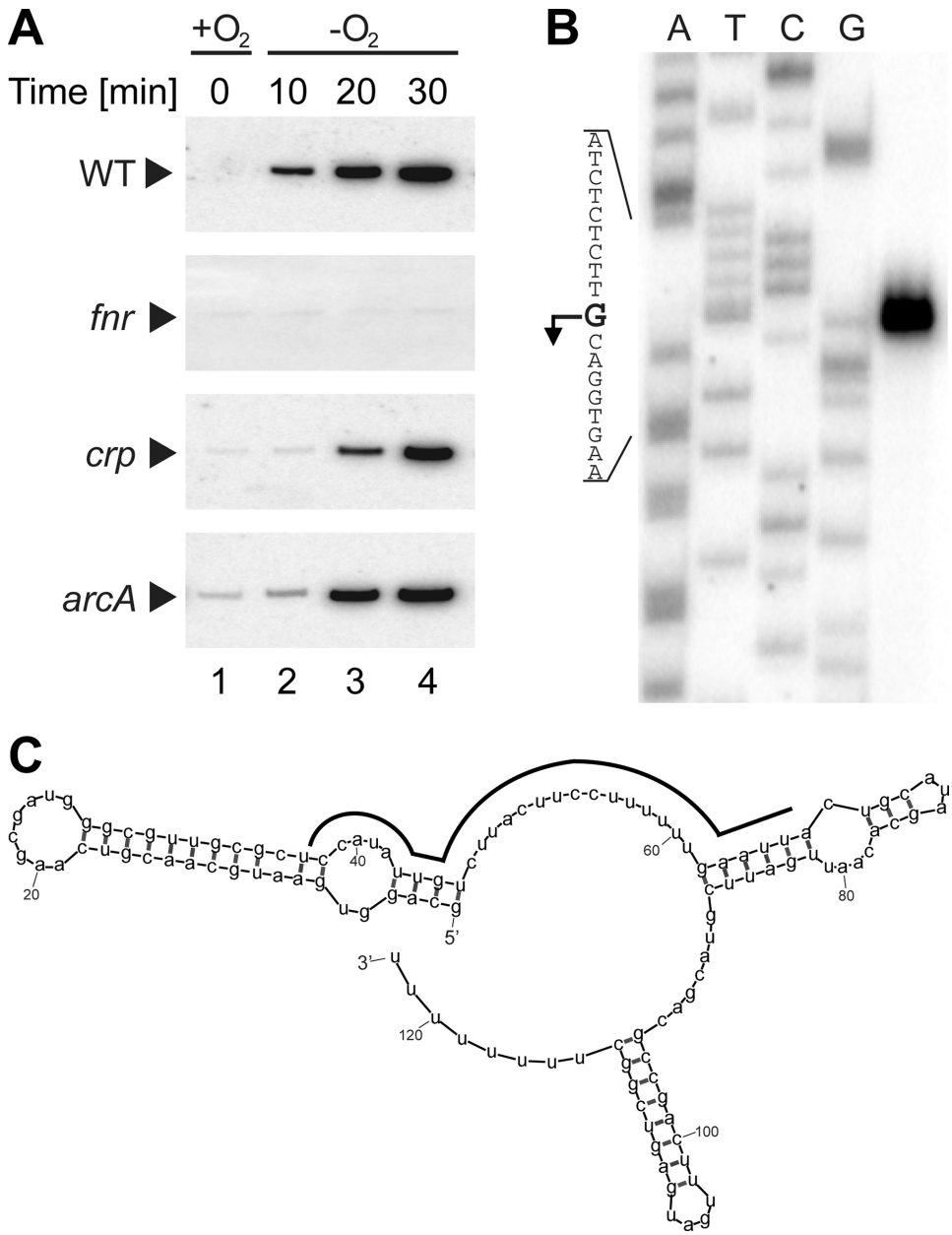

FIGURE 2. **Transcriptional regulation of *fnrS*.** *A*, shown is anaerobic regulation of FnrS RNA expression. Wild-type (*WT*) strain SØ928 and isogenic derivatives containing a chromosomal deletion of *fnr*, *crp*, or *arcA*, respectively, were grown with aeration in LB medium at 37 °C to exponential growth phase ($A_{450} \sim 0.3$). Samples were taken before (*lane 1*; 0 min) and after (*lanes 1–3*; 10, 20, 30 min) anaerobic incubation. The levels of FnrS were determined using Northern blot analysis. *B*, the transcription start site of the *E. coli fnrS* gene was determined by primer extension analysis with total RNA isolated from SØ928 grown under anaerobic growth conditions (*rightmost lane*). *C*, shown is the predicted secondary structure for *E. coli* FnrS from Mfold (67). The conserved segment of the sRNA that possesses sequence complementarity to the translational initiation region of target mRNAs as well as the predicted binding site for Hfq is marked by a *filled line*.

protecting it against endonucleolytic cleavage. We further measured the stability of the sRNA in the presence of ongoing transcription, which in the case of FnrS can be carried out simply by shifting from anaerobic to aerobic growth conditions (Fig. 3*C*). As found for a number of stress-induced small RNAs that act by an antisense mechanism (13, 17), FnrS was much more stable in cells in which transcription had been stopped by the antibiotic rifampicin than in cells with ongoing transcription (compare Figs. 3, *B* and *C*), suggesting that FnrS degradation was promoted by the presence of its target mRNAs. Similarly, a rapid turnover was observed in a strain carrying an ectopic copy of *fnrS* under tight control of the inducible $P_{A1/O4}$ *lac* promoter derivative (present on the R1 low copy number derivative pNDM-fnrS; *i.e.* in this background the production of the sRNA can be turned on/off very rapidly by adding or removing the inducer IPTG) (Fig. 3*D*).

Target Identification—Collectively the findings above hinted that FnrS RNA has roles in regulating target mRNAs via base pairing. Thus, in an attempt to further our understanding of the biological role of FnrS, we sought to identify putative target genes through genome-wide expression studies. Specifically, we examined the consequences of FnrS expression on mRNA abundance under two conditions. In the first set of experiments, the chromosomal copy of *fnrS* was deleted, and FnrS was expressed for 10 min from pNDM-fnrS during aerobic conditions and compared with cells carrying an empty pNDM220 vector. Under these conditions, we estimate that levels of FnrS were slightly higher (~2-fold) than that induced anaerobically from the chromosome. In the second set of experiments, the transcriptome of wild-type and FnrS-deficient cells was compared 30 min after a sudden shift to anaerobic conditions. In both sets of experiments, the strains were grown in LB at 37 °C; each experiment was carried out in triplicate. From the processed array intensity signals for all genes, a total of 48 genes displayed either increased (11) or decreased (37) expression levels (1.5-fold, $p < 0.05$) upon short term FnrS expression during aerobic condition (supplemental Table S3). Similarly, a total of 19 genes displayed either increased (16) or decreased (3) expression levels (1.5-fold, $p < 0.05$) in the *fnrS* deletion strain under anaerobic condition (supplemental Table S3). Only genes whose expression level changed reciprocally between the two conditions (*i.e.* decreased under the first condition and increased under the second condition) were considered as potential negative or positive targets of FnrS (Table 1).

Potential FnrS Targets—Of the 16 genes organized into 11 putative operons listed in Table 1, *sodB* and *gpmA* mRNAs dis-

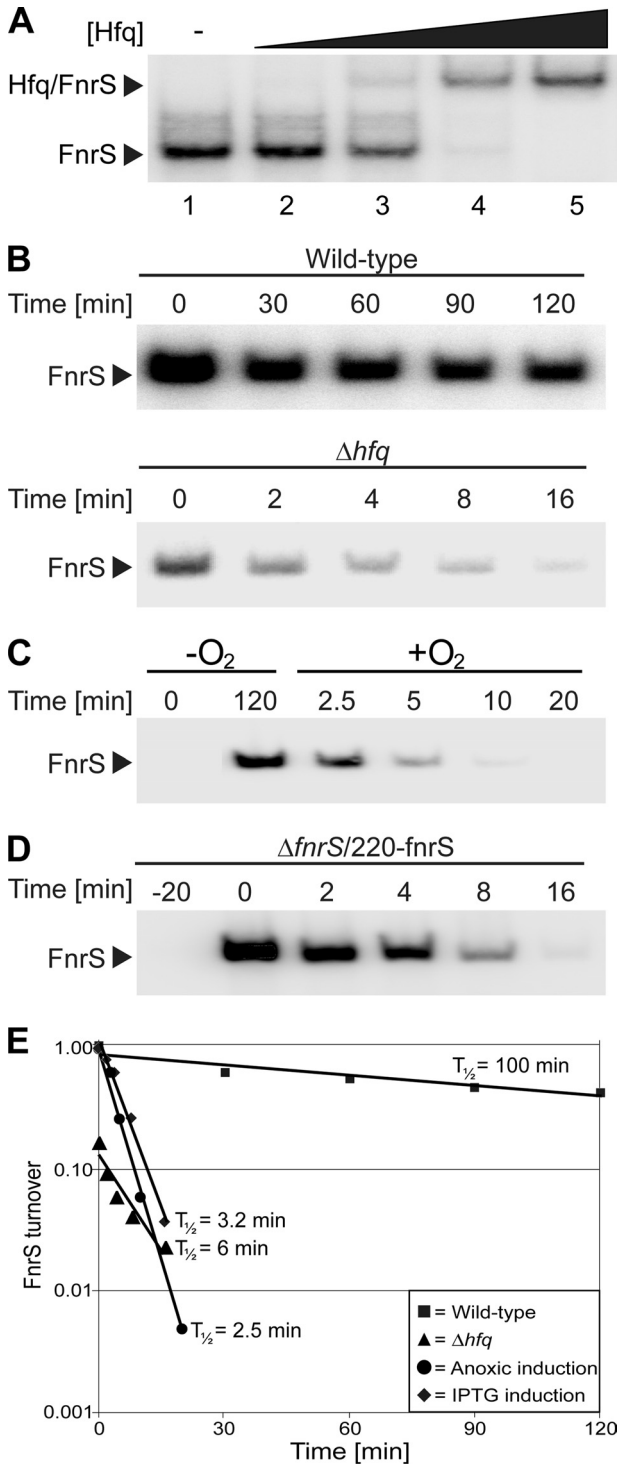

FIGURE 3. **Hfq binding and Northern blot analysis of FnrS stability in the absence and presence of ongoing transcription.** *A*, shown is a gel mobility shift assay of Hfq binding to FnrS RNA. Samples containing a 5′ end-labeled transcript of sRNA (4 nM final concentration) were incubated with increasing amounts of Hfq. Final hexameric concentrations of Hfq were 3.3 nM (*lanes 2*), 16.6 nM (*lanes 3*), 83.3 nM (*lanes 4*), and 333.3 nM (*lane 5*). No protein was added to the binding reaction (*lanes 1*). *B*, exponentially grown cultures of wild-type and Δ*hfq* strains were treated with rifampicin to block new transcription. Samples were taken at the indicated times, and total RNA was extracted. FnrS RNA levels were analyzed by Northern blot analysis. Estimated half-lives ($t_{1/2}$) are shown in *panel E*. *C*, shown is turnover of FnrS in the presence of ongoing transcription. Wild-type (SØ928) cells were grown anaerobically for 120 min, after which the culture was vigorously aerated. Samples were taken at the indicated times, and RNA was extracted and probed for FnrS. *D*, shown is decay of FnrS upon IPTG-controlled expression. Strain SØ928/Δ*fnrS*/pNDM220-fnrS was grown aerobically in LB with ampicillin (30 μg/ml) to an A_{450} of 0.4, and IPTG was added (1 mM final concentration) for 20 min The culture was centrifuged briefly to wash out the inducer and resuspended in an equal volume of prewarmed LB. Samples were taken at the indicated times, and RNA was extracted and probed for FnrS. *E*, shown is a graphical presentation of FnrS decay calculated from the experiments shown in *panels B*, *C*, and *D*. Full-length FnrS levels from the Northern blots were quantified and normalized as described under "Experimental Procedures."

played the most dramatic decrease in expression in response to FnrS overexpression, with a 4- and 5-fold decrease, respectively, in their mRNA levels (Table 1). *gpmA* encodes the glycolytic enzyme, phosphoglyceromutase 1, which catalyzes the interconversion of 2-phosphoglycerate and 3-phosphoglycerate, and *sodB* encodes an iron-containing superoxide dismutase (Fe-SOD), which removes O_2^-, a highly toxic form of oxygen. Intriguingly, the expression of both genes was shown to be repressed under anaerobic growth conditions in an FNR-dependent manner (32, 34); however, no well conserved FNR consensus binding site was found to be present in the promoter region of *gpmA* and *sodB*, leaving the regulation by FNR unexplained.

Several other FnrS-dependent genes/operons (*yobA*, *folE*, and *folX*) had previously been found to display FNR-dependent mRNA expression (32–34). Furthermore, the 5′-untranslated regions of *gpmA*, *sodB*, and *yobA* all display high sequence complementarity to a putative single-stranded region of FnrS RNA (Fig. 2*C* and supplemental Fig. S1). Thus, *gpmA*, *sodB*, and *yobA* are strong potential target candidates for antisense regulation by FnrS.

Among the negatively regulated FnrS target genes whose products are related to oxygen metabolism, we identified, in addition to *sodB*, genes of the *cydDC* operon (b0886 and b0887). This operon encodes an ATP-dependent transporter of glutathione required for maintaining balanced redox control in the periplasm and for assembling cytochrome *c* and periplasmic cytochrome *bd* (52, 53). Furthermore, the *yceJI* operon encodes a cytochrome b561 homolog that was reported to be negatively regulated by FNR (32–34). Only a single gene, *yhaO*, encoding a putative inner membrane transport protein, was found to be positively regulated by FnrS. However, expression of this gene has not been reported to be down-regulated anaerobically in strains lacking FNR. Taken together, our microarray data identified multiple potential targets for negative regulation by FnrS RNA.

Validation of Specific Targets—Selected targets from transcription profiling were examined further by Northern blot analysis. Among the potential direct targets was the *sodB* message, and consistent with the array data, short term induction of FnrS expression from plasmid pNDM-fnrS resulted in near complete elimination of this transcript in aerobically grown Δ*fnrS* cells (Fig. 4*A*, *left side*). In stark contrast, the Northern blot showed that the steady-state *sodB* mRNA level in an *hfq* deletion strain remained almost unaffected upon short term overexpression of the sRNA (Fig. 4*A*, *right side*). Thus, the FnrS-mediated regulation of *sodB* expression appears strictly dependent on Hfq, suggesting that the ribo-regulator acts by an antisense mechanism. Furthermore, as compared with wild-

TABLE 1
Potential FnrS regulated target genes

Gene	Blattner no.	Function	-Fold change[a] $+O_2$ $fnrS^{+++b}$ vs. $fnrS^{-}$	*p* Value	-Fold change[a] O_2 $fnrS^{-c}$ vs. wild type	*p* Value	FNR[d]-regulation and potential base-pairing[e]
FnrS-repressed target genes							
gpmA	b0755	Phosphoglyceromutase 1	−4.75	0.002	1.75	0.009	+,+
ybjC	b0850	Predicted inner membrane protein	−2.88	0.004	1.37	0.025	−,−
ybjB	b0851	Modulator of drug activity	−2.48	0.020	1.35	0.025	−,−
cydC[f]	b0886	Predicted inner membrane protein	−1.82	0.030	1.28	>0.05	+,−
cydD	b0887	ATP binding component of cytochrome-related transport	−2.79	0.007	1.57	0.033	+,−
yceI[f]	b1056	Base-induced periplasmic protein	−2.42	>0.05	2.58	0.002	+,−
yceJ	b1057	Predicted cytochrome b_{561}	−3.25	0.025	3.04	0.002	+,−
marA	b1531	Multiple antibiotic resistance transcriptional activator of defense systems	−2.46	0.028	1.55	0.010	+,−
sodB	b1656	Superoxide dismutase, iron	−3.72	0.018	1.71	0.000	+,+
yebY	b1839	Predicted protein	−3.59	0.003	2.45	0.008	+,−
yebZ	b1840	Putative resistance protein	−2.13	0.041	1.99	0.025	+,−
yobA[f]	b1841	Conserved protein	−1.39	>0.05	1.69	0.038	+,+
folE	b2153	GTP cyclohydrolase I	−2.51	0.003	1.48	0.044	+,−
folX	b2303	Dihydroneopterin triphosphate 2′-epimerase	−2.44	0.012	1.74	0.007	+,−
ytfJ	b4216	Conserved protein	−2.25	0.049	3.12	0.001	+,−
FnrS-activated target gene							
yhaO	b3110	Putative inner membrane transport protein	4.57	0.045	−2.41	0.003	−,−

[a] Positive -fold change denotes increasing gene expression levels compared to a reference, whereas negative -fold change denotes decreasing gene expression levels compared to a reference.
[b] $fnrS^{+++}$ *versus* $fnrS^{-}$ denotes aerobic ($+O_2$)-grown cultures subjected to ectopic *fnrS* pulse induction (10 min) from pNDM220-fnrS in $fnrS^{-}$ background compared to an isogenic reference strain containing a similarly induced empty vector.
[c] $fnrS^{-}$ *versus* wild type denotes anaerobic ($-O_2$, 30 min)-grown $fnrS^{-}$ culture compared to similarly treated wild-type reference.
[d] Negative anaerobic FNR regulation in any of Refs. 32–34.
[e] Sequence complementarity and possible base pairing between FnrS RNA and the TIR region of target mRNA.
[f] Genes located in the same operon as genes that pass the filtering criteria are included in the table if the direction of change of expression is consistent with the other gene(s) of the operon.

type cells, the *sodB* transcript increased over time in Δ*fnrS* cells upon a sudden shift to anaerobiosis (Fig. 4*B*).

FnrS possesses significant sequence complementarity to the translational initiation region (TIR) of *sodB*, and most of this pairing is conserved in several enterobacteria. Moreover, the *sodB* complementary region resides within a predicted single-stranded region of the sRNA (see Figs. 2*C* and 4*C*). To test whether FnrS might bind the complementary sequence in *sodB*-TIR, we performed gel mobility assays (Fig. 4*D*). When a constant amount of 5′ end-labeled FnrS RNA (2 nM) was incubated with increasing amounts of unlabeled RNA substrate carrying the *sodB* TIR, no or very little complex formation was observed in the absence of Hfq (Fig. 4*D*, *lanes 2–4*). In the presence of Hfq, however, complex formation was strongly enhanced; thus, at a *sodB* RNA concentration of 100 nM more than 90% of the binary FnrS-Hfq (*lane 5*) was shifted into a ternary FnrS-Hfq-*SodB*′ RNA complex (*lane 7*).

It seemed plausible, based on the results described above, that FnrS binds in an Hfq-dependent manner to the *sodB*-TIR, thereby leading to a reduction of the SodB protein synthesis rate and in a consecutive drop in the stability of the *sodB* mRNA. To substantiate this assumption, we employed a GFP-based plasmid system that specifically assays post-transcriptional regulation (40, 54). It involves ectopic co-expression of an sRNA and a translational gene fusion between a potential target mRNA sequence and the *gfp* gene. A key feature of the system is a constant transcription rate of both sRNA and target RNA, and therefore, only control at the post-transcriptional level is expected to affect the expression of the *gfp* fusion. Here, the 5′ end portion of *sodB*, spanning the 5′-untranslated region and the first 10 codons, was cloned into the low copy number *gfp* fusion vector pXG10. Transcription starts as in chromosomally encoded *sodB* gene and is driven by a constitutive λ_{PL} promoter derivative. The resulting plasmid was introduced in Δ*fnrS* cells harboring pNDM-fnrS or the empty vector pNDM220 (control), and transformants were grown aerobically in the presence of 1 mM IPTG for five to six generations before samples were taken for determination of the effects of FnrS expression on *sodB*′::*gfp* RNA and SodB::GFP protein synthesis by Northern and Western blot analysis, respectively. Note that we employed a single-copy vector rather than a high copy vector for sRNA expression (40). In addition, cell samples were examined from anaerobically grown cultures of wild-type and Δ*fnrS* strains harboring the pXG10-sodB::gfp expression plasmid. The results presented in Fig. 4*E* show that the cellular protein and mRNA levels under anaerobic growth conditions were increased (~2-fold) by deletion of the *fnrS* gene (compare *lanes 1* and *2*) and reduced ~3-fold under aerobic growth conditions by ectopic expression of the sRNA (compare *lanes 3* and *4*). On this basis we infer that FnrS specifically represses *sodB* expression by targeting the TIR region, most likely by an antisense mechanism.

Other potential targets identified in the array experiments included the *yobA-yebZY* operon and the *cydDC* genes encoding two glutathione ABC transporters that are important for maintenance of an optimum redox balance in the periplasm (Table 1). To validate FnrS-mediated negative regulation of these long operon transcripts, we employed primer extension analysis for the *cydDC* message. In accordance with the array data, the analysis revealed that the 5′ end portion of the transcript, starting at position −36 relative to the start codon, was rapidly reduced upon induction of *fnrS* expression under aerobic growth conditions while accumulating in Δ*fnrS* cells in response to anoxia (Fig. 5*A*). Collectively, these findings indicate that the *cydDC* mRNA is a direct target of FnrS.

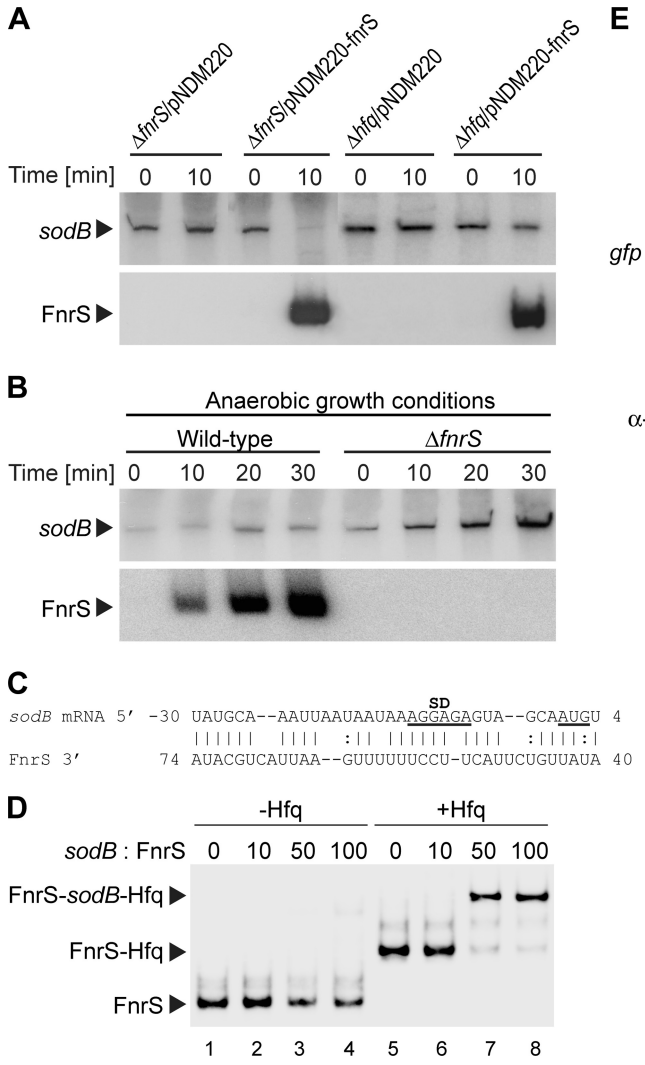

FIGURE 4. **FnrS-mediated repression of *sodB* expression and roles of Hfq.** *A*, strains SØ928Δ*fnrS*/pNDM220, SØ928Δ*fnrS*/pNDM220-fnrS, SØ928Δ*hfq*/pNDM220, and SØ928 Δ*hfq*/pNDM220-fnrS were grown aerobically in LB media to an A_{450} of 0.4 and then induced by the addition of IPTG (final concentration 1 mM). Samples were taken before (time 0), and 10 min after induction and total RNA was extracted. The *sodB* mRNA and FnrS RNA levels were analyzed by Northern blot. *B*, shown is accumulation of *sodB* mRNA in the absence and presence of FnrS RNA upon a sudden shift from aerobic to anaerobic growth. Aerobically grown cells of SØ928 and SØ928Δ*fnrS* were shifted to anoxia at time 0. Samples were taken at the indicated times, and RNA was extracted and probed for *sodB* mRNA and FnrS RNA. *C*, shown is putative base pairing between FnrS RNA and *sodB* mRNA. The translation start site is indicated. *D*, Hfq cooperates in RNA-RNA interaction. Samples containing 5′ end-labeled FnrS RNA (2 nM) and increasing amounts of unlabeled *sodB*′ RNA substrate (from −53 to + 97 relative to the translation start site) were incubated in the absence (*lanes 1–4*) or in the presence of Hfq (*lanes 5–8*), and complex formation was monitored in a electrophoretic mobility shift experiment. *sodB*′ RNA concentrations were as indicated, and the Hfq "hexamer" concentration was 0.33 μM. Unbound FnrS RNA and complexes corresponding to Hfq-FnrS RNA and FnrS RNA-Hfq-*sodB*′ RNA are indicated by *arrows*. *E*, target validation by translational *sodB*::*gfp* fusion is shown. In one experiment *E. coli* strains SØ928 and SØ928 Δ*fnrS* carrying the target fusion plasmid were grown anaerobically in LB media for at least six generations (A_{450} ~ 0.4) (*lanes 1* and *2*). In another experiment the Δ*fnrS*/pNDM220 and Δ*fnrS*/pNDM220-fnrS strains carrying target fusion plasmid were grown aerobically to an A_{450} of 0.4 in the presence of IPTG (1 mM final concentration) (*lanes 3* and *4*). For both experiments cells samples were subjected to Western blot analysis with monoclonal α-GFP antibodies (*upper panel*) and to Northern blot analysis of *gfp*-fusion mRNA and FnrS RNA (*second* and *third panels*). GroEL and 5S were used as loading control for Western and Northern blots, respectively.

Because the conserved single-stranded region of FnrS has extensive complementarity to the *yobA*-TIR and this putative pairing is retained in close relatives (supplemental Fig. S1), we examined post-transcriptional regulation of the *yobA-yebZY* mRNA by a translational pXG10-*yobA*′::*gfp* reporter fusion. This fusion encompasses nucleotides −150 to +30 relative to the ATG start codon of *yobA* mRNA, cloned in-frame with the *gfp* gene. As observed for the *sodB*′::*gfp* fusion, the absence of FnrS caused an increase in the level of the GFP fusion protein under anaerobic as well as aerobic growth conditions (*lanes 1* and *2* and *lanes 3* and *4*, Fig. 5*C*). In accordance with the array data for chromosomally encoded *yobA*, there was little effect of deleting the *fnrS* gene on the level of *yobA*′::*gfp* transcript (*second panel*; *lanes 1* and *2*); however, a significant reduction of this transcript was observed in cells that slightly overexpressed FnrS (*second panel*; compare *lanes 3* and *4*). These data together with the transcription profiling indicate that FnrS acts as an antisense RNA to repress the *yobA-yebZY* mRNA *in vivo* and suggest that the *yobA*-TIR is functionally relevant for this regulation.

Proteomics—In an attempt to identify additional targets for FnrS, we carried out proteomic profiling of the Δ*fnrS* strain harboring the control plasmid pNDM220 (empty vector) or the pNDM-fnrS vector. The two strains were grown aerobically under inducing conditions for at least five generations in LB medium, and then whole cell protein samples were collected and analyzed by SDS-PAGE. This identified SodA, the manganese-containing superoxide dismutase (Mn-SOD), as a protein whose synthesis is down-regulated in response to FnrS expression (data not shown). In addition, we performed a global analysis of protein expression changes after short term expression of the sRNA. In this approach the *fnrS* expression was induced for 30 min. After this, the cultures were pulse-labeled with [^{35}S]methionine and concentrated, and their proteins were analyzed by standard two-dimensional gel electrophoresis and autoradiography. Finally, those proteins whose synthesis rates was decreased after FnrS production were extracted, digested with trypsin, and analyzed by MALDI-TOF mass spectroscopy. This approach identified methionine synthase (MetE) and the leucine binding/transporter protein (LivK) as candidates for proteins whose production is negatively regulated by FnrS. In addition, the synthesis rate of glutamine-tRNA synthetase (GlnS) was up-regulated ~2-fold in response to FnrS expression (Fig. 6*A*).

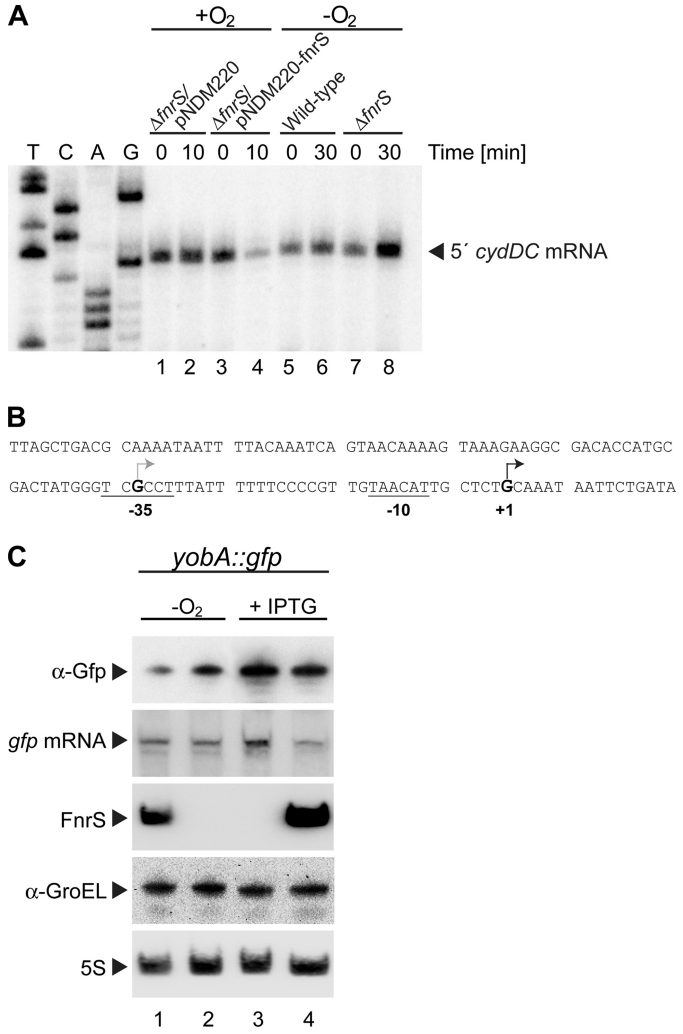

FIGURE 5. **FnrS-mediated repression of *cydDC* mRNA expression.** *A*, shown is primer extension analysis of *cydDC* 5′ end transcript. *fnrS* deletion strains containing an empty control vector (pNDM220) or pNDM220-*fnrS* were grown aerobically in LB medium at 37 °C to exponential growth phase (A_{450} ~ 0.3). Samples were taken before (*lanes 1* and *3*; 0 min) and after (*lanes 2* and *4*; 10 min) FnrS induction by 1 mM IPTG. Wild-type and *fnrS* deletion strains were grown aerobically in LB medium at 37 °C to exponential growth phase (A_{450} ~ 0.3). Samples were taken before (*lanes 5* and *7*; 0 min) and after (*lanes 6* and *8*; 30 min) of anaerobic incubation. *B*, the transcription start site (*black arrow*) was mapped to a position 33 bp downstream of the start site reported by Cook *et al.* (61) (*gray arrow*) (*i.e.* start site reassigned from position 930254 to 930221 of the *E. coli* chromosome). Putative −10 and −35 boxes are *underlined*. *C*, shown is validation of post-transcriptional regulation of the *yobA-yebZY* message by a translational *yobA*::*gfp* reporter fusion. The experiment as in Fig. 4*E* but with the pXG10-*yobA′*::*gfp* reporter plasmid.

To confirm the proteomic data, we carried out Northern analysis for *sodA* mRNA. Induced expression of FnrS from plasmid pNDM-fnrS resulted in a rapid reduction in this transcript (Fig. 6*B*, *left panel*), and the absence of FnrS resulted in a slower and less efficient down-regulation in response to anoxia (Fig. 6*B*, *right panel*). In binding studies, complex formation between FnrS and a *sodA* RNA substrate encompassing the TIR proceeds slowly without Hfq but very rapidly in its presence (Fig. 6*C*), and also in this case the conserved single-stranded region of the sRNA possesses significant complementarity to the TIR of the *sodA* mRNA (supplemental Fig. S1). Consistent with these findings, the absence of FnrS caused an increase in anaerobic expression of a pXG10-*sodA′*::*gfp* protein fusion (sequences −51 to + 30 of *sodA* joined to *gfp*) (~1.4-fold), and vice versa, the overexpression of the sRNA resulted in greater than 2-fold reduction in protein as well as in mRNA expression from the *sodA′*::*gfp* fusion (Fig. 6*D*). Taken together these findings suggest that FnrS is also an antisense regulator of Mn-SOD synthesis.

Finally, we investigated effects of FnrS on MetE synthesis, the most strongly affected spot on two-dimensional gels upon short term overexpression of FnrS (Fig. 6*A*). As a base-pairing interaction can be predicted between the conserved single-stranded region of FnrS and the *metE* TIR (supplemental Fig. S1) and most of the complementarity is retained in several enterobacteria, we constructed a *metE′*::*gfp* protein fusion that encompasses the region from −169 to +30 relative to the start of the *metE* gene. When slightly overexpressed, the sRNA down-regulated aerobic mRNA and protein expression of this fusion by 2.5-fold, and an *fnrS* deletion strain showed a significant increase (~2-fold) in protein as well as mRNA levels in anaerobic expression of the fusion (Fig. 6*E*). Thus, the *metE* transcript is likely a direct target for the anaerobically induced sRNA. Consistently, anaerobically *sodA* as well as *metE* expression was known to be negatively regulated by FNR though an undetermined mechanism (32, 34).

DISCUSSION

Enteric bacteria such as *E. coli* and *Salmonella* are highly versatile chemoheterotrophs that can use a wide variety of growth substrates under aerobic and anaerobic conditions, generating energy from either fermentation or aerobic or anaerobic respiration. Many of these catabolic pathways are controlled in response to the availability of oxygen and alternative electron acceptors at the level of gene expression Moreover, many of the metabolic transitions between aerobic and anaerobic states are controlled at the transcription level, primarily by the activities of two anaerobically activated gene regulatory systems composed of FNR and ArcA/B (26). A primary role for FNR is to coordinate carbon and energy metabolism under anaerobic growth conditions, and results from global gene expression profiling revealed that a very large number of genes (~200 operons) directly or indirectly are controlled by FNR (32–34).

In the present work we have identified a novel member of the FNR regulon, the conserved Hfq-binding sRNA FnrS. The transcription of this RNA species is strictly dependent on FNR, and thus, it can hardly be detected in cells deleted for the *fnr* gene or in cells grown aerobically. The results of stability experiments revealed that FnrS, like several well studied stress-induced sRNAs, was much more stable in the absence than in the presence of ongoing transcription, suggesting that it acts by an antisense mechanism and that FnrS decay is coupled to that of its mRNA target(s). Accordingly, we employed global proteomic and transcriptomic profiling for identification of putative target RNAs. To discriminate between direct and indirect effects of FnrS expression, two different conditions were employed. First, a long term effect of sRNA expression was investigated by comparing the transcriptome of wild-type and *fnrS* deletion strains during anaerobic growth. Second, the consequence of controlled

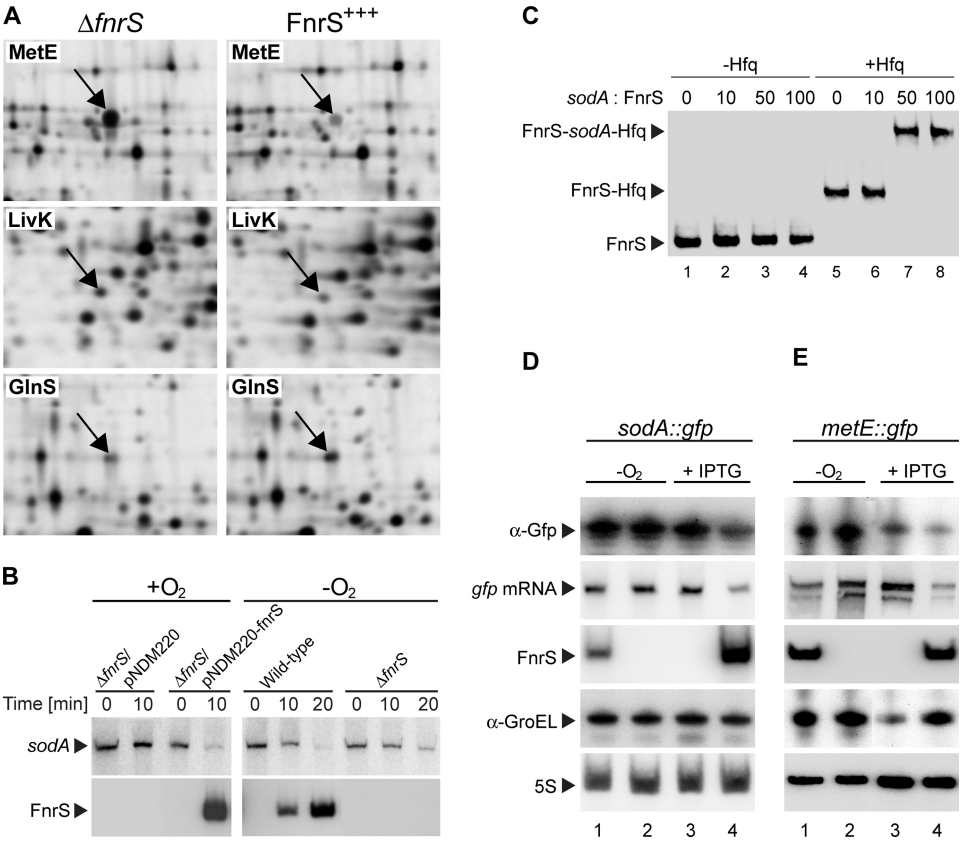

FIGURE 6. **Effect of *FnrS* expression on the protein pattern of *E. coli*.** *A*, the figure shows the relevant part of two-dimensional gels of strains Δ*fnrS*/pNDM220 (control) and Δ*fnrS*/pNDM220-fnrS. Cells were grown to log phase in minimal medium supplemented with glucose and then induced with 0.5 mM IPTG for 30 min at 37 °C. After this the cultures were labeled with [^{35}S]methionine for 2 min and concentrated by centrifugation, and their proteins were analyzed by standard two-dimensional gel electrophoresis and autoradiography. The *arrows* indicate the position of proteins whose net synthesis rate was markedly altered upon FnrS expression. *B*, *left panel*, FnrS mediated repression of *sodA* expression. Strains SØ928Δ*fnrS*/pNDM220 (control) and SØ928Δ*fnrS*/pNDM220-fnrS were grown aerobically in LB media to an A_{450} of 0.4 and then induced by addition of IPTG (final concentration 1 mM). Samples were taken before (time 0) and 10 min after induction, and total RNA was extracted. The *sodA* mRNA and FnrS RNA levels were analyzed by Northern. *B*, *right panel*, shown is the effect of *fnrS* deletion on *sodA* expression. Aerobically grown cells of SØ928 and SØ928Δ*fnrS* were shifted to anoxia at time 0. Samples were taken at the indicated times, and RNA was extracted and probed for *sodA* mRNA and FnrS RNA. *C*, Hfq cooperates in RNA-RNA interaction. Samples containing 5′ end-labeled FnrS RNA (2 nM) and increasing amounts of unlabeled $sodA_{1-150}$ substrate (covering the transcription start site to 97 nucleotides downstream of the translation start site) were incubated in the absence (*lanes 1–4*) or in the presence of Hfq (*lanes 5–8*), and complex formation was monitored in a electrophoretic mobility shift experiment. *sodA*′ RNA concentrations were as indicated, and the Hfq hexamer concentration was 0.33 μM. Unbound FnrS RNA and complexes corresponding to Hfq-FnrS RNA and FnrS RNA-Hfq-*sodA*′ RNA are indicated by *arrows*. *D*, shown is validation of post-transcriptional regulation of *sodA* expression by a translational *sodA*::*gfp* reporter fusion. The experiment was as in Fig. 4*E* but with the pXG10-*sodA*′::*gfp* reporter plasmid. *E*, the experiment was the same as *D* but with pXG10-*metE*′::*gfp* reporter plasmid.

short term expression of FnrS on the transcriptome/proteome was examined in the *fnrS* deletion strain grown aerobically. By focusing on genes whose expression levels changed reciprocally between the two conditions, the mRNA profiling resulted in 11 differentially expressed transcripts of which 10 were regulated negatively by FnrS. Notably, in independent work by Durand and Stortz (55), 9 of the latter transcripts were also found to be down-regulated after FnrS overexpression in whole genome expression analysis. Furthermore, our proteome analyses resulted in three negatively and one positively regulated candidate targets. Finally, we validated the regulation of five of the repressed targets by one or more independent experiment(s). In the following we will discuss these targets in the context of their metabolic roles and their expression patterns reported in previous studies.

The expression of several genes connected to oxygen utilization is down-regulated or switched off in response to anoxia. A well studied example is Mn-SOD (coded for by the *sodA* gene) that protects cells from oxidative damage by removing superoxide radicals, a highly toxic form of oxygen produced as an inadvertent byproduct during the reduction of O_2 to H_2O in respiration. First, ArcA represses *sodA* transcription in anaerobiosis, coupling its expression to aerobic respiration (56). Second, characterization of regulatory mutations that caused moderate anaerobic derepression of *sodA*::*lacZ* protein fusions identified FNR as an additional negative regulator of *sodA* expression that increases the down-regulation further (~6-fold) (56, 57). In addition to the gene regulatory studies, anaerobic gene expression profiling in *E. coli* K-12 revealed elevated expression of the *sodA* gene (2.4–2.8-fold) in FNR-deficient strains compared with wild-type (32, 33). However, no obvious sequences that resemble the FNR consensus sequence seemed to be present in the *sodA* promoter region, suggesting that FNR-mediated repression of this gene is indirect (57, 58). In line with these data, we found that the cellular level of *sodA* message was down-regulated upon a sudden shift to anoxia and that the down-regulation was significantly more efficient in the presence than in the absence of FnrS (Fig. 6*B*, *right panel*). Furthermore, we observed that the *sodA* mRNA level rapidly declined upon short term controlled induction of FnrS. In addition, we found that complex formation between FnrS and the TIR region of the *sodA* transcript proceeds very slowly without Hfq but readily in its presence. These results together with repression studies of a GFP-based target fusion (Fig. 6*D*) led us to propose that the anaerobic repression of *sodA* expression by FNR is mediated post-transcriptionally by FnrS.

In a similar manner we validated the FnrS-mediated down-regulation of the expression of *sodB*, encoding the alternative cytoplasmic superoxide dismutase, Fe-SOD, that contains iron rather than manganese. In prior studies no transcriptional control of the *sodB* gene was observed, but the *sodB* mRNA level has been found to be elevated 28-fold (34) and 2.4-fold (32, 33)

by deleting the *fnr* gene of *E. coli* strains grown anaerobically in LB and glucose minimal medium, respectively. In agreement with a direct physical interaction between FnrS and the *sodB*-untranslated region, we found that sRNA regulation *in vivo* as well as duplex formation *in vitro* were compromised in the absence of Hfq (Fig. 4). Furthermore, a translational control by FnrS is consistent with the fact that no DNA binding site for FNR was observed in the *sodB* promoter region. Clearly, the "oxidative" function of SodA and B provides a logic rationale for down-regulating their production under anaerobic conditions, and a translational regulation that can be switched off rapidly might be advantageous against sudden exposures to oxygen.

A *sod*A/B double mutant mutates spontaneously at a very high rate and is severely compromised in aerobic survival. Thus, the presence of two highly homologous superoxide dismutases has been attributed to differences in regulation and/or roles in oxidative stress (59). In this context expression of both *sod* genes is under control of the Fur protein, which in the presence of sufficient iron represses the transcription of genes involved in iron assimilation. Under such conditions *sodA* transcription is partially repressed by Fur, and Sod enzyme is mainly produced from the *sodB* locus. When iron becomes scarce, Fur becomes inactive, resulting in derepression of *sodA* transcription; however, only under conditions in which FNR and ArcA are inactive (*i.e.* in presence of O_2). Hence, Fur has no effect on anaerobic transcription of *sodA* (56, 58). In contrast, SodB production is down-regulated when iron becomes scarce, as expression of the *sodB* locus is controlled negatively at the post-transcriptional level by the Fur-repressed small RNA RyhB (5, 17); *i.e.* when Fur repression becomes inactive, RyhB is rapidly expressed, and the sRNA pairs with *sodB*-TIR in an antisense manner, which blocks translation (60). Clearly, the presence of two differentially regulated *sod* genes allows the cell to produce adequate amounts of enzyme under various growth/stress conditions. In addition, the *sod* regulatory case provides an interesting example of Fur regulation of a "non-iron" protein as well as a significant example of dual sRNA control of a single target RNA.

The two operon candidate transcripts, *cydDC* and *yobA-yebZY*, were previously considered to be repressed by FNR (32, 61). In gene expression profiling, *cydDC* showed a ~2-fold and *yobA-yebZY* showed a ~3-fold increase under anaerobic conditions in FNR-deficient strains (32, 33) and, thus, display regulatory patterns very similar to those observed in an FnrS-deficient strain (Table 1). Potential FNR binding sites have been recognized in the promoter regions of both operons (32, 61). In *cydD-P* the site (5′-TTGATN$_4$AaCgc-3′, where lowercase letters are used to indicate bases that do not match the FNR site consensus) is centered 123 bp upstream of the transcription initiation site (Fig. 5*B*). However, a mutation in *fnr* did not affect anaerobic expression of an Φ(*cydD-lacZ*) operon fusion, suggesting that FNR repression is indirect and mediated at the post-transcriptional level (61). In agreement with this view, we observed a marked decrease in the 5′ end portion of *cydD* mRNA upon short term induction of FnrS expression (Fig. 5*A*). CydDC proteins are responsible for transport of glutathione from the cytoplasm to the periplasmic space for maintenance of the optimum redox balance in this compartment (52, 53), and therefore, it would make biological sense to down-regulate these transporters when the environment becomes depleted for oxygen.

In the *yobA* promoter region the putative DNA site for FNR (5′-TTGATgatccTCgAc-3′) is centered 67 bp upstream of the translation start site, but the transcription initiation site has not yet been examined. Thus, further analysis is necessary to determine whether FNR directly regulates the expression of this operon. However, it is clear from the *yobA*::*gfp* fusion studies that FnrS negatively affects production of fusion protein as well as fusion transcript. Based on this finding and the fact that FnrS has extensive complementarity to the *yobA*-TIR (supplemental Fig. S1) it would seem safe to predict that FnrS acts by an antisense mechanism to down-regulate *yobA-YebZY* expression.

Among negatively regulated candidate transcripts, *gpmA* displayed the highest amount of regulation (~5-fold, Table 1). Similarly, *gpmA* was previously found to be repressed by FNR; however, no potential FNR binding site was recognized in the *gpmA* promoter region (32, 61). Currently, we are exploring the FnrS-mediated regulation of the production of the glycolytic enzyme GpmA under different growth conditions, including anaerobic respiration as well as the molecular mechanism for shutting off its production. In this regard FnrS down-regulation of *gpmA* mRNA as well as four additional targets (*i.e. marA*, *folE*, *folX*, and *sodB*) was validated in parallel by Durand and Stortz (55).

Finally, by proteomics we identified two proteins engaged in transport or synthesis of amino acids whose production was decreased upon short term induction of *fnrS* transcription. The most strongly affected synthesis rate was for MetE (Fig. 6*A*, *top*), and data from *in vivo* expression assays for a *metE*::*gfp* translational reporter fusion were indicative of translational control (Fig. 6*E*). In support of this view, previous studies demonstrated that *metE* expression exhibits a 5-fold increase under anaerobic conditions in an FNR-deficient strain (32), and after the transition from anaerobic to aerobic growth in minimal medium, wild-type cells were found to rapidly induce *metE* mRNA and MetE protein synthesis (62, 63). Furthermore, the conserved single-stranded region of FnrS and the *metE*-TIR have potential for base-pairing, and the complementarity is retained in relatives such as *Salmonella*, *Klebsiella*, and *Citrobacter* (supplemental Fig. S1). Regarding a biological role of the FnrS-mediated regulation, it has been established that the biosynthetic enzymes MetE and GTP cyclohydrolase (FolE) (also a potential target, see Table 1) are among the proteins most susceptible to oxidation in *E. coli* (64, 65). In fact, there is experimental evidence suggesting that MetE oxidation poses problems, resulting in methionine starvation, during the transition from anaerobic to aerobic growth (63). Thus, the FnrS-mediated control may play a role in rapid adaptation to anaerobic-aerobic transitions.

In summary, we have identified a conserved anaerobically induced small regulatory RNA that plays a significant role in FNR-mediated gene regulation at the post-transcriptional level. Specifically, our results revealed that the sRNA down-regulates the expression of various classes of genes ranging from genes with aerobic functions to genes with housekeeping functions in

energy production and biosynthesis. Our findings expand the list of global regulators known to control sRNA expression, thereby reinforcing the assumption that all major regulons are likely to include at least one small RNA regulator (3, 66).

Acknowledgments—We thank Adelina Rogowska-Wrzesinska for assistance with two-dimensional gel electrophoresis and Gisela Storz for sharing unpublished information.

REFERENCES

1. Bartel, D. P. (2009) *Cell* **136,** 215–233
2. Vogel, J. (2009) *Mol. Microbiol.* **71,** 1–11
3. Waters, L. S., and Storz, G. (2009) *Cell* **136,** 615–628
4. Altuvia, S., Weinstein-Fischer, D., Zhang, A., Postow, L., and Storz, G. (1997) *Cell* **90,** 43–53
5. Massé, E., Salvail, H., Desnoyers, G., and Arguin, M. (2007) *Curr. Opin. Microbiol.* **10,** 140–145
6. De Lay, N., and Gottesman, S. (2009) *J. Bacteriol.* **191,** 461–476
7. Møller, T., Franch, T., Højrup, P., Keene, D. R., Bächinger, H. P., Brennan, R. G., and Valentin-Hansen, P. (2002) *Mol. Cell* **9,** 23–30
8. Papenfort, K., Pfeiffer, V., Lucchini, S., Sonawane, A., Hinton, J. C., and Vogel, J. (2008) *Mol. Microbiol.* **68,** 890–906
9. Johansen, J., Eriksen, M., Kallipolitis, B., and Valentin-Hansen, P. (2008) *J. Mol. Biol.* **383,** 1–9
10. Delihas, N., and Forst, S. (2001) *J. Mol. Biol.* **313,** 1–12
11. Guillier, M., and Gottesman, S. (2006) *Mol. Microbiol.* **59,** 231–247
12. Valentin-Hansen, P., Johansen, J., and Rasmussen, A. A. (2007) *Curr. Opin. Microbiol.* **10,** 152–155
13. Moon, K., and Gottesman, S. (2009) *Mol. Microbiol.* **74,** 1314–1330
14. Hammer, B. K., and Bassler, B. L. (2007) *Proc. Natl. Acad. Sci. U.S.A.* **104,** 11145–11149
15. Vanderpool, C. K. (2007) *Curr. Opin. Microbiol.* **10,** 146–151
16. Aiba, H. (2007) *Curr. Opin. Microbiol.* **10,** 134–139
17. Massé, E., Escorcia, F. E., and Gottesman, S. (2003) *Genes Dev.* **17,** 2374–2383
18. Valentin-Hansen, P., Eriksen, M., and Udesen, C. (2004) *Mol. Microbiol.* **51,** 1525–1533
19. Arluison, V., Hohng, S., Roy, R., Pellegrini, O., Régnier, P., and Ha, T. (2007) *Nucleic Acids Res.* **35,** 999–1006
20. Rasmussen, A. A., Johansen, J., Nielsen, J. S., Overgaard, M., Kallipolitis, B., and Valentin-Hansen, P. (2009) *Mol. Microbiol.* **72,** 566–577
21. Soper, T. J., and Woodson, S. A. (2008) *RNA.* **14,** 1907–1917
22. Zhang, A., Wassarman, K. M., Ortega, J., Steven, A. C., and Storz, G. (2002) *Mol. Cell* **9,** 11–22
23. Brennan, R. G., and Link, T. M. (2007) *Curr. Opin. Microbiol.* **10,** 125–133
24. Link, T. M., Valentin-Hansen, P., and Brennan, R. G. (2009) *Proc. Natl. Acad. Sci. U.S.A.* **106,** 19292–19297
25. Schumacher, M. A., Pearson, R. F., Møller, T., Valentin-Hansen, P., and Brennan, R. G. (2002) *EMBO J.* **21,** 3546–3556
26. Guest, R. J., Green, J., Irvine, A. S., and Spiro, S. (1996) in *Regulation of Gene Expression in Escherichia coli* (Lin, E. E. C., and Simon Lynch, A., eds) pp. 317–337, R. G. Landes Co., Austin, TX
27. Compan, I., and Touati, D. (1994) *Mol. Microbiol.* **11,** 955–964
28. Georgellis, D., Kwon, O., and Lin, E. C. (2001) *Science* **292,** 2314–2316
29. Khoroshilova, N., Popescu, C., Münck, E., Beinert, H., and Kiley, P. J. (1997) *Proc. Natl. Acad. Sci. U.S.A.* **94,** 6087–6092
30. Lazazzera, B. A., Beinert, H., Khoroshilova, N., Kennedy, M. C., and Kiley, P. J. (1996) *J. Biol. Chem.* **271,** 2762–2768
31. Li, B., Wing, H., Lee, D., Wu, H. C., and Busby, S. (1998) *Nucleic Acids Res.* **26,** 2075–2081
32. Constantinidou, C., Hobman, J. L., Griffiths, L., Patel, M. D., Penn, C. W., Cole, J. A., and Overton, T. W. (2006) *J. Biol. Chem.* **281,** 4802–4815
33. Kang, Y., Weber, K. D., Qiu, Y., Kiley, P. J., and Blattner, F. R. (2005) *J. Bacteriol.* **187,** 1135–1160
34. Salmon, K., Hung, S. P., Mekjian, K., Baldi, P., Hatfield, G. W., and Gunsalus, R. P. (2003) *J. Biol. Chem.* **278,** 29837–29855
35. Sawers, R. G., Zehelein, E., and Böck, A. (1988) *Arch. Microbiol.* **149,** 240–244
36. Sambrook, J., Fritsch, E. F., and Maniatis, T. (1989) *Molecular Cloning. A Laboratory Manual*, 3rd Ed., Appendix A2.4, Cold Spring Harbor Laboratory Press, Cold Spring Harbor, NY
37. Clark, J. D., and Maaløe, O. (1967) *J. Mol. Biol.* **23,** 99–112
38. Datsenko, K. A., and Wanner, B. L. (2000) *Proc. Natl. Acad. Sci. U.S.A.* **97,** 6640–6645
39. Gotfredsen, M., and Gerdes, K. (1998) *Mol. Microbiol.* **29,** 1065–1076
40. Urban, J. H., and Vogel, J. (2007) *Nucleic Acids Res.* **35,** 1018–1037
41. Saeed, A. I., Bhagabati, N. K., Braisted, J. C., Liang, W., Sharov, V., Howe, E. A., Li, J., Thiagarajan, M., White, J. A., and Quackenbush, J. (2006) *Methods Enzymol.* **411,** 134–193
42. Overgaard, M., Johansen, J., Møller-Jensen, J., and Valentin-Hansen, P. (2009) *Mol. Microbiol.* **73,** 790–800
43. Franch, T., Gultyaev, A. P., and Gerdes, K. (1997) *J. Mol. Biol.* **273,** 38–51
44. Melville, S. B., and Gunsalus, R. P. (1996) *Proc. Natl. Acad. Sci. U.S.A.* **93,** 1226–1231
45. Overgaard, M., Borch, J., Jørgensen, M. G., and Gerdes, K. (2008) *Mol. Microbiol.* **69,** 841–857
46. Mortz, E., Krogh, T. N., Vorum, H., and Görg, A. (2001) *Proteomics* **1,** 1359–1363
47. Rogowska-Wrzesinska, A., Larsen, P. M., Blomberg, A., Görg, A., Roepstorff, P., Norbeck, J., and Fey, S. J. (2001) *Comp. Funct. Genomics* **2,** 207–225
48. Prokhorova, T. A., Nielsen, P. N., Petersen, J., Kofoed, T., Crawford, J. S., Morsczeck, C., Boysen, A., and Schrotz-King, P. (2006) *Vaccine* **24,** 6446–6455
49. Wassarman, K. M., Repoila, F., Rosenow, C., Storz, G., and Gottesman, S. (2001) *Genes Dev.* **15,** 1637–1651
50. Grainger, D. C., Aiba, H., Hurd, D., Browning, D. F., and Busby, S. J. (2007) *Nucleic Acids Res.* **35,** 269–278
51. Sittka, A., Lucchini, S., Papenfort, K., Sharma, C. M., Rolle, K., Binnewies, T. T., Hinton, J. C., and Vogel, J. (2008) *PLoS Genet.* **4,** e1000163
52. Pittman, M. S., Robinson, H. C., and Poole, R. K. (2005) *J. Biol. Chem.* **280,** 32254–32261
53. Poole, R. K., Gibson, F., and Wu, G. (1994) *FEMS Microbiol. Lett.* **117,** 217–223
54. Urban, J. H., and Vogel, J. (2009) *Methods Mol. Biol.* **540,** 301–319
55. Durand, S., and Storz, G. (2010) *Mol. Microbiol.*, in press
56. Compan, I., and Touati, D. (1993) *J. Bacteriol.* **175,** 1687–1696
57. Beaumont, M. D., and Hassan, H. M. (1993) *J. Gen. Microbiol.* **139,** 2677–2684
58. Hassan, H. M., and Sun, H. C. (1992) *Proc. Natl. Acad. Sci. U.S.A.* **89,** 3217–3221
59. Hopkin, K. A., Papazian, M. A., and Steinman, H. M. (1992) *J. Biol. Chem.* **267,** 24253–24258
60. Geissmann, T. A., and Touati, D. (2004) *EMBO J.* **23,** 396–405
61. Cook, G. M., Membrillo-Hernández, J., and Poole, R. K. (1997) *J. Bacteriol.* **179,** 6525–6530
62. Smith, M. W., and Neidhardt, F. C. (1983) *J. Bacteriol.* **154,** 336–343
63. Partridge, J. D., Scott, C., Tang, Y., Poole, R. K., and Green, J. (2006) *J. Biol. Chem.* **281,** 27806–27815
64. Leichert, L. I., and Jakob, U. (2004) *PLoS Biol.* **2,** e333
65. Hondorp, E. R., and Matthews, R. G. (2004) *PLoS Biol.* **2,** e336
66. Gottesman, S. (2005) *Trends Genet.* **21,** 399–404
67. Zuker, M. (2003) *Nucleic Acids Res.* **31,** 3406–3415